

Phase Reactions Between Refractory and High-Acidic Synthetic CaO-Ferronickel Slag

CHRISTOPH SAGADIN,^{1,4} STEFAN LUIDOLD,^{1,5} CHRISTOPH WAGNER,²
ALFRED SPANRING,² and THOMAS KREMMER³

1.—CD Laboratory for Extractive Metallurgy of Technological Metals, Montanuniversitaet Leoben/Nonferrous Metallurgy, Franz-Josef-Straße 18, 8700 Leoben, Austria. 2.—RHI Feuerfest GmbH-Nonferrous Metals, Wienerbergerstraße 9, 1100 Vienna, Austria. 3.—Montanuniversitaet Leoben / Nonferrous Metallurgy, Franz-Josef-Straße 18, 8700 Leoben, Austria. 4.—e-mail: christoph.sagadin@unileoben.ac.at. 5.—e-mail: stefan.luidold@unileoben.ac.at

Interactions between high melting synthetic ferronickel slags with acidic character and MgO as refractory were investigated. In order to facilitate the complex composition of real ferronickel slag, a synthetic slag of SiO₂-MgO-Fe₂O₃-CaO was used. The practical corrosion tests of the MgO refractory were performed in a hot-stage microscope at temperatures of 1650°C under a CO/CO₂ atmosphere for process-oriented conditions. The formed phases between slag and magnesia substrate were analyzed by scanning electron microscope analysis. The results show that, by penetrating the slag into the refractory, the melt dissolves the magnesia and forms Mg- and Ca silicates. Furthermore, a diffusion of Fe from the slag into the magnesia grains can be observed and a transformation to magnesiowustite occurs. Thermodynamic phase calculations using FactSage software confirmed the generation of these minerals. The combination of practical testing and thermodynamic calculations should ultimately provide a path for improving the refractory lifetime and performance.

INTRODUCTION

Refractory stability is an essential factor in the ferroalloy industry especially for ferronickel production. The corrosion of the refractory caused by high melting slags massively influences the furnace life-time. Reduced production efficiency and furnace shutdowns are some of the results of inferior refractory. Therefore, the aim is to select adequate furnace linings for individual processes to provide homogeneous wear and predictable refractory service limits for scheduled maintenance and high furnace availability.¹⁻³

The chemical attack of the refractory by metal, slag, dust and atmosphere constitutes an important cause of corrosion. This leads to the disintegration of refractory furnace walls with simultaneous penetration by liquid substances, which could change the mechanical stability. The resistance of the refractory against corrosion can be achieved by suitable measures during the production of the furnace lining or by proper process management.

The chemical reactivity of the liquid slag composed of ions plays a key role in metallurgical processes. The deterioration can be described by a four-stage process: wetting, which is followed by penetration due to porosity, disruption of the refractory bonds by chemical reactions, and finally erosion of the refractory constituents by flowing liquids. Therefore, the right choice of refractories with high corrosion and erosion resistance is one of the critical requirements to be satisfied. During the manufacture of ferronickel, temperatures of more than 1650°C and high acidic slags are typical for the smelting process, which stresses the ceramic magnesia refractory despite its high melting point, good mechanical properties at elevated temperatures and ability to withstand hostile conditions.²⁻⁸

According to Hu,⁹ basic magnesia refractory material has a higher resistance performance than acidic refractories in the ferronickel process despite the acidic slags. In detail, FeO and MgO form a substitution solid solution resulting in a decreased FeO content in the slag system. Consequently, the

Table I. Chemical analysis of synthetic slag (ICP-OES, titration for valence of Fe-ions) and magnesia substrate

Chemical analysis	(wt.%)										
	SiO ₂	MgO	CaO	Al ₂ O ₃	Fe _{tot}	Fe ²⁺	Fe ³⁺	Fe ₂ O ₃	BD	AP	CTE
Synthetical slag	49.3	18.7	4.25	–	19.1	6	13.1	–	–	–	–
Refractory substrate	< 0.35	> 99.3	< 0.35	< 0.25	–	–	–	< 0.12	2.3	35	13

BD bulk density (g/cm³), *AP* apparent porosity (wt.%), *CTE* coefficient of thermal expansion (10⁻⁶/K).

viscosity of the slag increases and penetration would decline.⁹ Investigations of corrosion mechanisms are commonly performed by using a range of simplified laboratory-scale experiments.^{10,11} The current tests combine practical measurements in laboratory-scale trials with theoretical thermodynamic calculations to understand the actual corrosion mechanisms, which is necessary for an improvement of the refractory performance and lifetime. The focus of this work is the evaluation of corrosion of refractory substrates and phase formation when a synthetically produced slag, based on data from FeNi producers, interacts with them. Therefore, the slag is melted in a hot-stage microscope under a defined CO/CO₂ gas mixture to mimic actual process conditions. Further, the examinations include investigations via scanning electron microscopy (SEM) for phase determination and thermodynamic calculation by using FactSage 7.1¹² software. The characterization of the corrosion of refractories by combining hot-stage microscopy and SEM including energy dispersive x-ray spectroscopy (EDX) with thermodynamic calculations provides an important basis for the further development of the ferronickel process and therefore applied refractory.

METHODS AND MATERIALS

Hot-Stage Microscope

Usually, a hot-stage microscope (HSM) is applied for investigations of the sintering and deformation temperature as well as the melting behavior of different materials like slags, dusts and ashes. The HSM (EM301; Hesse Instruments, Germany) consists of several main components: a halogen lamp, a high-temperature tube furnace, a CCD camera and a control unit. It is a complete testing system designed to determine high-temperature characteristics such as wetting angle, softening behavior and spherical or hemispherical points of the specimen materials. In the current research, the HSM served as the melting and reaction device. Therefore, a slag powder was pressed into a 3-mm-high and 3-mm-diameter slag cylinder, which was positioned on a small magnesia refractory substrate. With a

controlled heating rate of 10 K/min, the tube furnace was heated to 1700°C, which correlates to a sample temperature of 1650°C. The slag sample melts, infiltrates and reacts with the magnesia substrate at this temperature. One hour after reaching 1650°C, the furnace was automatically switched off and cooled to room temperature. To mimic the real ferronickel process in the laboratory-scale test, a gas mixture of 60 vol% CO and 40 vol% CO₂ was used as atmosphere, corresponding to an oxygen partial pressure of 1.94×10^{-7} atm at 1650°C (calculated by FactSage). The furnace purging of the reducing gas mixture amounted to 0.16 l/min, which is about twice the furnace volume.

Sample Preparation and SEM/EDX Analysis

After the investigation in the hot-stage microscope, the magnesia substrate including the melted and infiltrated slag was cut in cross-section by a diamond grinding wheel. Then, the sample was embedded in a two-component resin (resin with hardener, Araldite DBF). A smooth sample surface was achieved by grinding in several steps with different SiC foils (800, 1200, 2400 and 4000). A thin film of sputtered carbon made the sample surface conductive, which is essential for scanning electron microscopy.

The microstructure of the slag/refractory interface was analyzed by a SEM (JEOL JSM IT-300 LV) equipped with an EDX analyser. The measurements took place with the following imaging conditions: 20 kV, scan time: 800 μs/pixel, resolution: 2048 × 2048, approximate counts on mapping: 8×10^5 on main element, 1.5×10^6 counts in sum.

Thermodynamic Analysis

To understand the processes of interaction between synthetic FeNi slag and magnesia refractory, thermodynamic calculations were carried out with FactSage 7.1 software. The calculations were performed by using the modules Phase Diagram and Equilib as well as the databases FactPS and FToxide. The main focus of the thermodynamic investigations is to simulate refractory attack by slag and its comparison with experimental results.

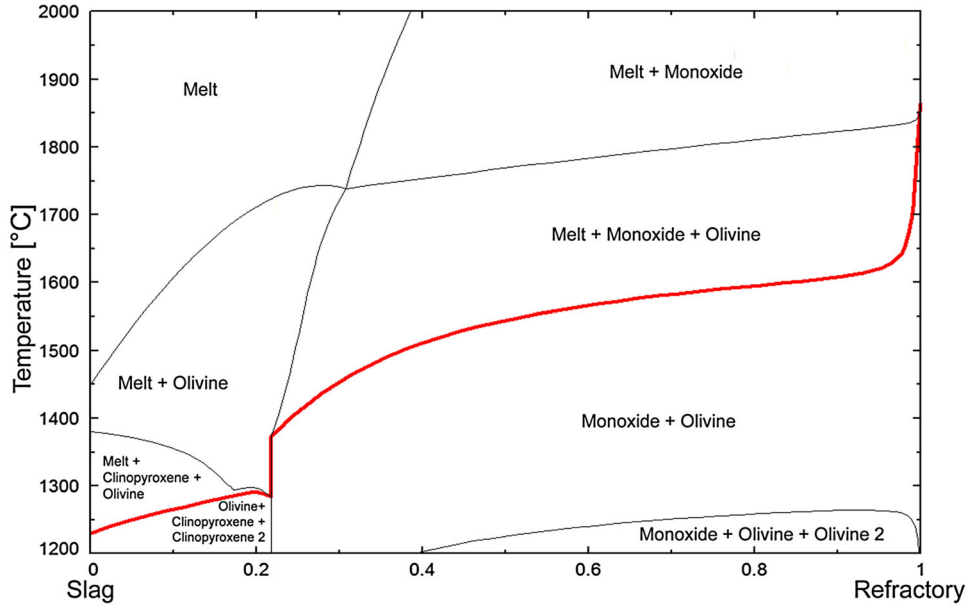


Fig. 1. Slag/refractory system (calculated with FactSage) in reducing atmosphere of 60% CO and 40% CO₂.

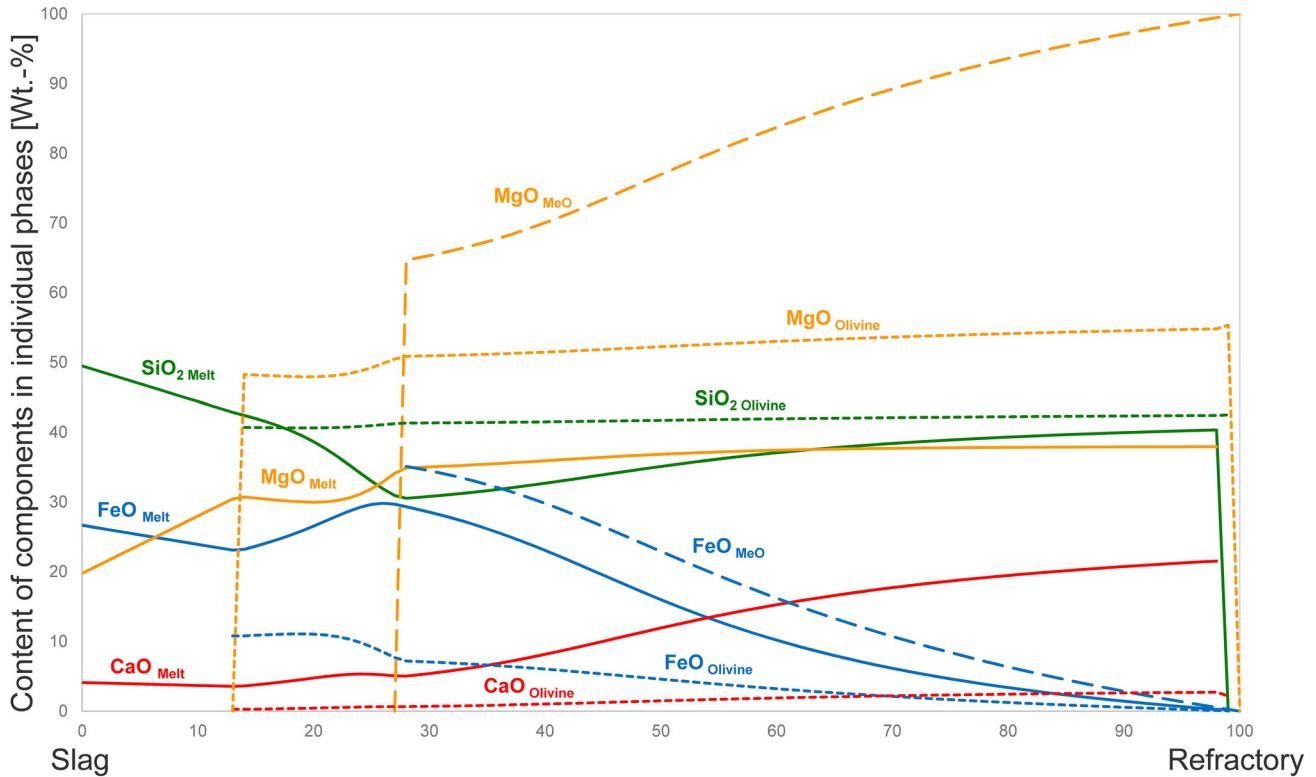


Fig. 2. Content of particular components in phases at 1650°C.

Materials

SiO₂, MgO, Fe₂O₃ and CaO constitute the oxides for the production of the synthetic slag. The mixture of oxides as received, each with more the 99% purity (i.e. composed of 48% SiO₂, 19.2% MgO, 28.8% Fe₂O₃ and 4% CaO) was homogenized and melted in

a graphite crucible by an induction furnace. After the casting of the melt, the solid slag was ground in a swing mill to produce a fine slag powder. Table I shows the chemical analysis of the high-quality magnesia plate (14 × 14 × 2 mm) and of the synthetic slag produced.

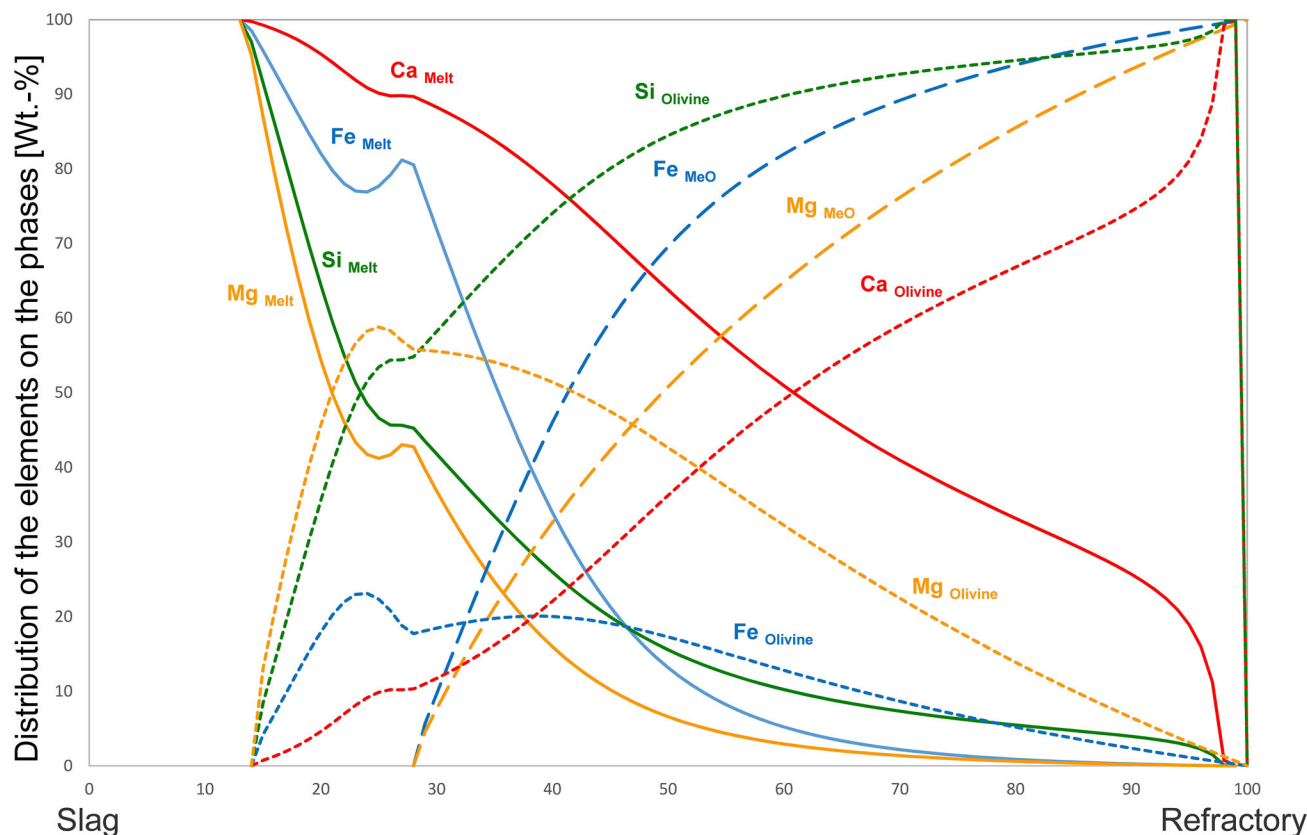


Fig. 3. Distribution of the elements Fe, Mg, Si and Ca on the phases olivine, monoxide (MeO) and melt at 1650°C in an atmosphere of 60% CO and 40% CO₂.

Thermodynamic Calculations

The thermodynamic calculation of stable phases at the slag/refractory interface with FactSage is a main part of this research. The corrosion phase model ranges from pure slag (48% SiO₂, 19.2% MgO, 28.8% Fe₂O₃ and 4% CaO) to pure magnesia (MgO). The calculation was performed for the same atmosphere (60% CO and 40% CO₂) as used by the practical corrosion test in the HSM. In Fig. 1, the stable phases at thermodynamic equilibrium between the slag and refractory material are displayed as a function of refractory/slag portion and temperature. This is approximately comparable with the phase diagrams for MeO_x-MgO-SiO₂ in the slag atlas.¹³

An isotherm section at 1650°C of the slag/refractory-system is displayed in Fig. 2, which illustrates the distribution of the components in the phases. At a low refractory to slag ratio of up to 13%, the slag consists of a melt and dissolves the refractory, then the first-phase olivine becomes thermodynamically stable. The calculations predict that the silicate called olivine is composed of MgO, SiO₂, FeO and CaO. The chemical composition of the olivine is approximately constant in the stability zone, except that FeO decrease with an increasing refractory content. At about 27% refractory, the next phase,

magnesiowuestite (MeO), appears which consists of the dominating components MgO and FeO. This phase has a solid solution range from pure FeO to pure MgO where the liquidus temperature significantly increases with rising MgO content. The concentration of Fe₂O₃ in the melt is not illustrated in the diagram due to its too small content. At 0% slag the ratio of Fe₂₊/Fe₃₊ is about 72 and decreases to a ratio of 12 at about 27% refractory and to 9 at even higher refractory fractions.

Figure 3 illustrates the distribution of the elements on individual thermodynamically stable phases as a function of the refractory/slag ratio. The bulk of Mg and Si forms an olivine phase between 13% and 27% refractory in the mixture, whereas Fe and Ca primarily remain in the melt. As soon as the monoxide phase reaches stability, the Fe content of olivine and melt rapidly decreases. The expulsion of Fe and Mg from the olivine causes an intensified enrichment of Ca in the olivine on the basis of exchangeability of Ca, Fe and Mg ((Mg,Fe,Ca)₂SiO₄).

SEM/EDS Corrosion Evaluation

In addition to the thermodynamic calculations, microstructure investigations were carried out by SEM/EDX. Figure 4 shows a section of the slag/

refractory transition from the slag to the pure refractory. The upper zone indicates the infiltration of slag into the refractory. The slag-influenced zone is approximately 350–450 μm thick, however, the infiltration depth can vary depending on the open porosity of substrate. The corresponding spot analyses are summarized in Table II.

Figure 5 exhibits the element distribution of Mg, Si, Fe and Ca of the slag/refractory intersection. It shows a qualitative measurement of these elements, wherein brighter-colored regions correspond to a higher element concentration.

Equilibrium Calculation for Slag/Refractory Interfaces

The equilibrium calculation between two neighboring phases express an important point. For the correlation of the experimentally determined compositions with the phase diagram, the Fe/Mg ratios in olivine and magnesiowustite were calculated over the complete slag/refractory range by FactSage. The measured Fe/Mg ratio of region A from Fig. 4 amounts to 0.1 for olivine (solidified infiltrated slag)

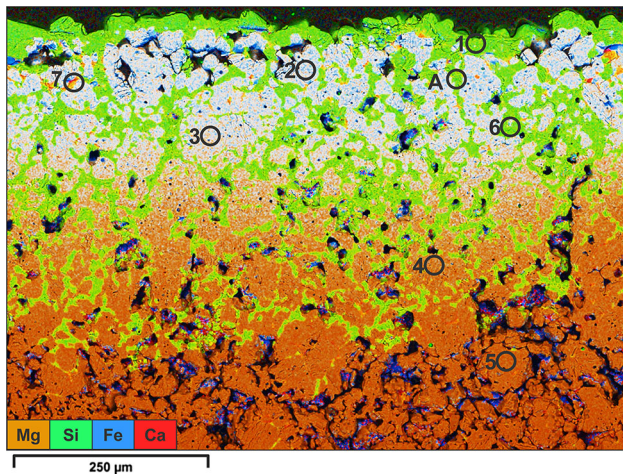


Fig. 4. EDX mapping with spot analyses at the slag/refractory intersection.

and 0.35 for monoxide (MgO grains with absorbed FeO). The thermodynamic calculations were done for a temperature of 1400°C, which describes the approximate consistency to the practical corrosion test. Figure 6 illustrates the measured Fe/Mg ratios as well as the calculated ones as a function of the slag/refractory mixture.

RESULTS AND DISCUSSION

The results of the melting trials regarding the slag/refractory intersection show good agreement with thermodynamic calculations. The matrix consists of slag and refractory, where the slag fills up the pores of the refractory. At the beginning, the slag infiltrates the substrate along the pores, reacts and partly dissolves the refractory. Large MgO grains of the refractory are not dissolved by the slag. Fe ions from the slag diffuse into the MgO particles and form magnesiowustite (Mg, Fe)O, meanwhile, the slag dissolves some magnesia and builds the silicate olivine. The olivine ((Mg,Fe,Ca)₂SiO₄) comprises of Mg, Ca and Fe, which are exchangeable, and Si.

The mapping (Fig. 4) shows different ranges of element concentrations: areas composed of magnesiowustite (white) indicated by the presence of Mg, Fe and O; areas containing of Si, Mg, Fe, Ca and O (green) and areas comprising of Mg and O (orange). Spots 1 and 6 indicate high Si concentrations in the slag. They exhibit (Mg, Fe, Ca)/Si ratios of approximately 2 (2.2 at EDX spot) which coincide with the stoichiometry of olivine. The chemical analyses of the EDX spots show contents of Fe and Ca similar to the thermodynamic analysis. A high FeO_x content in the slag causes a highly enrichment of MgO with Fe oxide. The analyses on the refractory grains (Spots 2, 3, 4 and 5) reveal a decreasing Fe content from top to bottom. The formed magnesiawustite corresponds to the phase monoxide of the thermodynamic FactSage database, FToxide. Spot 7 represents a high Ca-containing phase, which was not attributable to the results of thermodynamic calculations for 1650°C.

Table II. Proportions and ratios of oxide cations

Element (mol.%)	EDX spot						
	1	2	3	4	5	6	7
Mg	64.5	87.1	90.2	96.6	98.7	64.5	28.9
Si	31.6	–	0.7	–	–	31.6	20.9
Fe	3.4	12.9	9.2	3.4	1.3	2.4	6.8
Ca	0.5	–	–	–	–	1.6	43.4
(Mg, Fe, Ca)/Si ratio	2.2	–	–	–	–	2.2	3.8
Mg/Fe	18.7	6.7	9.9	28.8	76.2	27.2	4.3

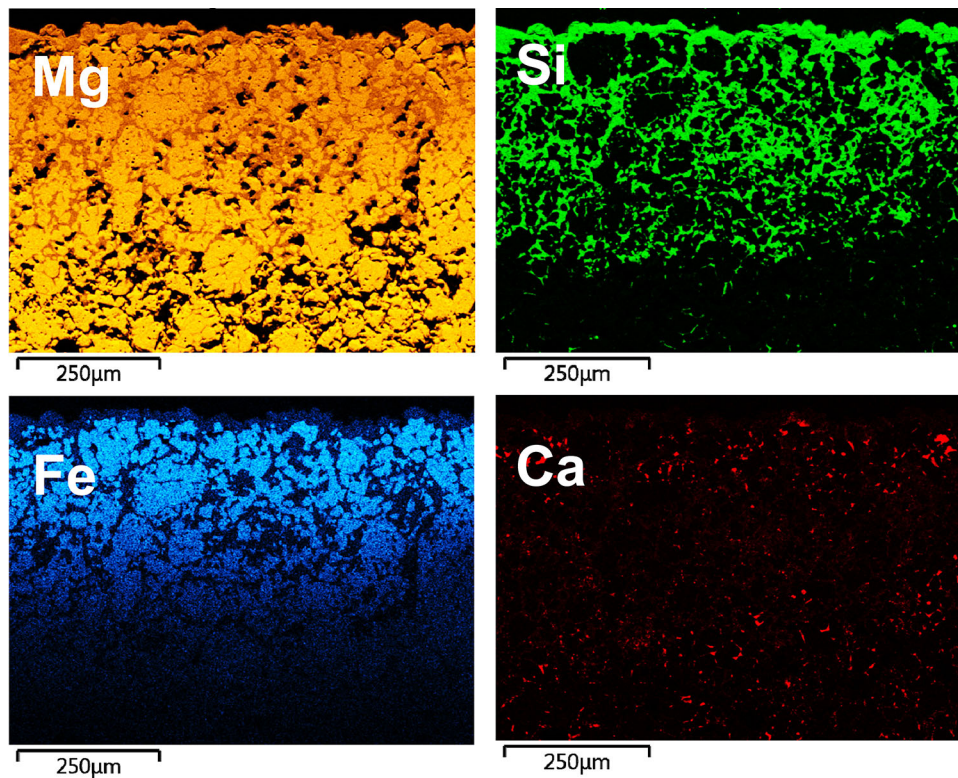


Fig. 5. Distribution of Mg, Si, Fe and Ca of the slag/refractory intersection analyzed by SEM/EDX.

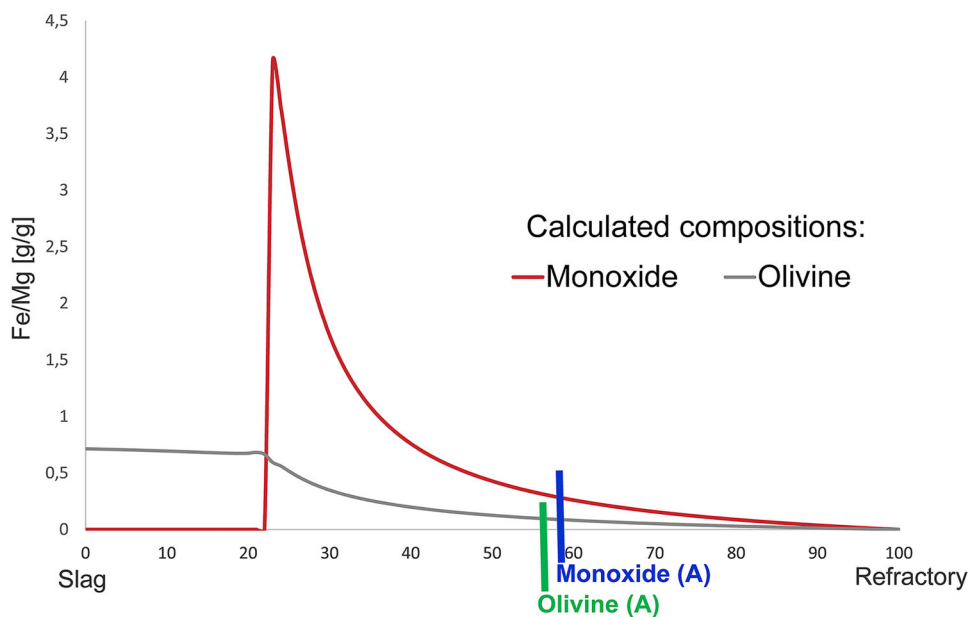


Fig. 6. Equilibrium between slag (olivine) and refractory (monoxide) in comparison to measurements of spot A in Fig. 4.

The equilibrium calculation of spot A indicates that the composition of the analysed olivine matches to the calculation results for 55% refractory in the mixture and that of monoxide to 57.5% refractory.

That means that the two neighboring phases (olivine and magnesiowustite) are close to the equilibrium (in balance when they are arranged at the same position).

CONCLUSION

The very acidic high melting ferronickel slags challenge ferronickel and refractory producers. To achieve an understanding how the corrosion mechanisms at the slag/refractory interface act in ferronickel manufacturing, an analysis of the microstructure is unavoidable and constitutes the main topic of this work. The combination of theoretical and experimental investigation methods, namely hot-stage microscopy, inclusive SEM/EDX analysis and thermodynamic FactSage calculations provides excellent results.

The thermodynamic calculations were carried out for the main oxides (FeO_x , MgO and SiO_2) and CaO (slag in contact with refractory) as a function of temperature. The formed phases at the slag/refractory intersection was the main focus of attention. The outcome from the practical investigation methods showed good agreement with the thermodynamic phase calculations.

The corrosion is caused by penetration of the molten slag and reaction with the refractory substrate. It results in the formation of new phases and a partial dissolution of the magnesia substrate.

The thermodynamic calculations are a suitable tool for predicting the sequence of phase transformations in equilibrium and are, therefore, useful for supporting experimental investigations. The future work involves corrosion mechanisms of real refractory substrates by different ferronickel slag systems, where the presented methodology will be refined and extended.

ACKNOWLEDGEMENTS

Open access funding provided by Montanuniversitaet Leoben. The financial support by the Austrian Federal Ministry of Science, Research and Economy and the National Foundation for Research, Technology and Development is gratefully acknowledged.

OPEN ACCESS

This article is distributed under the terms of the Creative Commons Attribution 4.0 International License (<http://creativecommons.org/licenses/by/4.0/>), which permits unrestricted use, distribution, and reproduction in any medium, provided you give appropriate credit to the original author(s) and the source, provide a link to the Creative Commons license, and indicate if changes were made.

REFERENCES

1. F.K. Crudwell, M.S. Moats, V. Ramachandran, T.C. Robinson, and W.G. Davenport, *Extractive Metallurgy of Nickel, Cobalt and Platinum-Group Metals* (Amsterdam: Elsevier, 2011), pp. 49–93.
2. C. Wagner, C. Wenzl, D. Gregurek, D. Kreuzer, S. Luidold, and H. Schnideritsch, *Metall. Mater. Trans. B* 49B, 116 (2017).
3. C. Sagadin, S. Luidold, C. Wagner, and C. Wenzl, *JOM* 68, 3022 (2016).
4. S. Luidold, C. Wenzl, C. Wagner, and C. Sagadin, *MOLTEN16. in Proceedings of 10th International Conference on Molten Slags, Fluxes and Salts*, p. 53, 2016.
5. F. Harders and S. Kienow, *Feuerfestkunde: Herstellung, Eigenschaften und Verwendung feuerfester Baustoffe* (Heidelberg/Berlin: Springer, 1960), pp. 150–159.
6. C. Sagadin, S. Luidold, C. Wenzl, and C. Wagner, *TMS 2017. in Proceedings of 8th International Symposium on High-Temperature Metallurgical Processing*, p. 161, 2017.
7. L. Rodd, N. Voermann, F. Stober, S. Lee, K. Lim, J. Yoo, S. Roh, and J. Park, *INFACON XII 2010. in Proceedings of the Twelfth International Ferroalloys Congress*, p. 697, 2010.
8. V. Sharapova, *Refract. Ind. Ceram.* 51, 374 (2011).
9. D. Hu, P.X. Liu, and S.J. Chu, *INFACON XIV 2015. in Proceedings of the Fourteenth International Ferroalloys Congress*, p. 115, 2015.
10. D. Gregurek, A. Ressler, V. Reiter, A. Franzkowiak, A. Spanring, and T. Prietl, *JOM* 65, 1622 (2013).
11. M. Wang, C. Hsu, and M. Hon, *Ceram. Int.* 35, 1501 (2009).
12. C.W. Bale, E. Belicic, P. Chartrand, S.A. Decterov, G. Eriksoon, K. Hack, I.-H. Jung, Y.-B. Kang, J. Melancon, A.D. Pelton, C. Robelin, and S. Petersen, *CALPHAD Comput. Coupling Ph. Diag. Thermochem.* 33, 295 (2009).
13. Verein Deutscher Eisenhüttenleute, *Slag Atlas*, 2nd ed. (Düsseldorf: Verlag Stahleisen, 1995), p. 142.